Response Time of a Plasmonic Distributed Feedback Laser in a Large-Signal Modulation Regime

N.E. Nefedkin,[1,2,3,*] A.A. Zyablovsky,[1,2] E.S. Andrianov,[1,2] A.A. Pukhov,[1,2,3] and A.P. Vinogradov[1,2,3]

[1] *Dukhov Research Institute of Automatics (VNIIA), 22 Sushchevskaya, Moscow 127055, Russia*

[2] *Moscow Institute of Physics and Technology, Moscow 141700, Russia*

[3] *Institute for Theoretical and Applied Electromagnetics, 13 Izhorskaya, Moscow 125412, Russia*

(Received 7 February 2019; revised manuscript received 4 April 2019; published 24 May 2019)

The time response to an external signal is the main characteristic of optoelectronic devices that determines their maximum modulation frequency. The use of plasmonic structures provides the opportunity to significantly reduce the response time. In this paper, we study the temporal dynamics of a plasmonic distributed feedback laser consisting of a two-dimensional metallic structure coated with a layer of the active medium. Combining numerical simulations with an analytical evaluation, we show that the response time in the large-signal modulation regime strongly depends on the size of the pump beam. We demonstrate that the interaction of a large number of modes of the plasmonic structure with the pumped active medium leads to the formation of a single collective mode. If the size of the pump beam is larger than the propagation length of electromagnetic waves in the plasmonic structure, the collective mode is localized in the pumped area. In this case, the response time slightly increases with the size of the pump beam. In the opposite case, the mode is not localized inside the pumped area and the response time increases with the narrowing of the beam. We demonstrate that there is a minimum size of the pump beam for which the modulation speed is a maximum, and can achieve 1 THz. The results obtained opens the way to increasing both the modulation speed and the energy efficiency of plasmonic laser devices.

DOI: 10.1103/PhysRevApplied.11.054067

I. INTRODUCTION

For many optoelectronic applications, such as the modulation of optical signals and sensing, lasers with an ultrafast modulation response are required [1,2]. Such devices often operate in a large-signal modulation regime where a pumping pulse switches the laser between the subthreshold regime and the above-threshold regime. In such a scheme the response of the laser to a pumping pulse can be divided into three stages [3–5]. First, the response is initiated by spontaneous emission in the active medium, which creates the electromagnetic (EM) field in the cavity. In the second stage, the stimulated emission begins to prevail over the spontaneous emission and the intensity of the EM field in the cavity rapidly increases, while the population inversion of the active medium decreases. When the population inversion has vanished, the growth of the EM-field intensity ceases and the third stage begins. The EM-field intensity drops due to losses in the cavity.

During the first stage, the intensity of the EM field in the cavity is negligible, and only in the second stage does a significant response to the external pumping pulse appear. Hence the duration of the first stage determines the delay time of the output pulse. It can be reduced by accelerating the spontaneous emission by an increase of the Purcell factor [3,4]. To achieve a high Purcell factor, one can use a large Rabi constant of the interaction between the electric field and the active medium. In turn, the increase of the Rabi constant leads to an increase of the rate of stimulated emission and a decrease of the duration of the second stage. The duration of the third stage is determined by the relaxation rate of the EM field in the cavity. Thus, to create a short output pulse, one has to work in the high-Purcell regime to reduce the delay time, and use cavities with a high relaxation rate to shorten the third stage and narrow the width of the pulse.

The maximal modulation frequency of surface-emitting lasers based on dielectric structures is limited to several tens of gigahertz [6,7]. This frequency can be significantly increased if one use metallic plasmonic structures. The localization of the EM field at the nanoscale results in a strong interaction with the atoms of the active medium and, as a consequence, a high Purcell factor. Losses in the metal cause a high relaxation rate of the EM field of the plasmonic structure. Both of these factors lead to an increase of the modulation speed. At the same time, the use of periodic structures enables the achievement of desirable radiation losses and beam directionality of plasmonic lasers. These

*nefedkin@phystech.edu

arguments have stimulated significant interest in the creation and study of lasers based on plasmonic nanoparticle arrays or perforated films [2,8–10], particularly in the large-signal modulation regime [1].

Periodicity inevitably results in the multimode nature of these lasers [8,11]. As a result, the excited active medium emits in many modes simultaneously. This leads to a decrease in the energy in each mode and a delay of the second stage, in which stimulated emission dominates. Consequently, the total response time increases, which may limit the advantages of the use of plasmonic structures. Thus, the question arises of the possibility of overcoming the difficulties associated with the multimode nature of plasmonic lasers.

In this paper, we study the dynamics in the large-signal modulation regime of a plasmonic distributed feedback (DFB) laser that consists of a gold film perforated by a periodic array of holes and coated with a layer of an active medium. We examine the behavior of the laser for different sizes of the pump beam. Combining numerical simulations of the laser dynamics within the framework developed in Refs. [12,13] with an analytical evaluation, we show that the response time strongly depends on the size of the pump beam. This dependence is due to the complex structure of the modes of the DFB laser. The interaction of the laser modes with the pumped active medium causes the emergence of a single collective mode whose properties strongly depend on the pump-beam size. If the pump beam is larger than the decay length of the EM field in the plasmonic structure, the collective mode is localized inside the pumped area. The response time in this case reaches picoseconds and practically does not change with the size of the pump beam. In the opposite case, the mode is not localized inside the pumped area and the response time increases with the narrowing of the beam. Consequently, there is a diameter of the pump beam, d^*_{beam}, necessary to achieve the shortest response time. This diameter is about the decay length of the EM field in the plasmonic structure, and for the plasmonic laser considered it is approximately 15 μm. When the size of the pump beam is greater than d^*_{beam}, the response time of the plasmonic laser is approximately 1 ps. The results obtained confirm that plasmonic DFB lasers can have a modulation frequency exceeding several hundred gigahertz in the large-signal modulation regime. Optimization of the size of the pump beam allows an increase in the modulation speed, as well as in the energy efficiency of plasmonic DFB-laser devices.

II. TEMPORAL DYNAMICS OF A TWO-DIMENSIONAL PLASMONIC DFB LASER

A conventional plasmonic DFB laser consists of a periodic plasmonic structure (e.g., a metallic film perforated by an array of holes [8,10,11,13–17] or two-dimensional arrays of plasmonic nanoparticles [1,2,9,18–22]) and an active medium. The eigenmodes of such a system are Bloch modes that are distributed over the whole surface of the laser. To overcome losses in the metal, external pumping (optical or electrical) of the active medium is used. In the case of optical pumping, the diameter of the pump beam is usually smaller than the size of the periodic plasmonic structure [1,2,15] (see Fig. 1). In such a case, the EM field is excited inside the pumped area and is formed by a large number of Bloch modes [13,15]. To describe the multimode dynamics of the plasmonic DFB laser we use an approach proposed in Ref. [12] for considering ultrafast phenomena in dispersive dissipative media. This approach is based on the following equations:

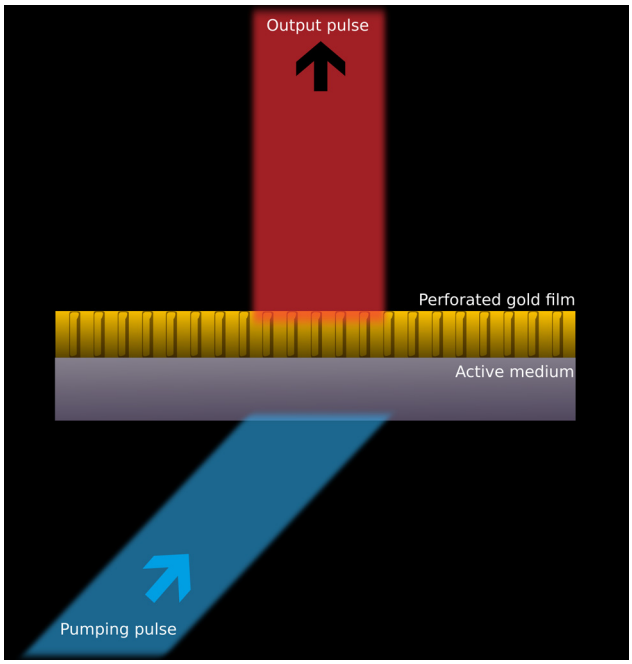

FIG. 1. The two-dimensional plasmonic distributed feedback laser. The diameter of the holes is 160 nm, the distance between the holes is 470 nm, and the thickness of the Au film is 100 nm.

$$\frac{dn_{jk}}{dt} = -\left(\gamma_j + \gamma_k\right) n_{jk} + i\left(\omega_j - \omega_k\right) n_{jk} + \sum_{m=1}^{N_{\text{atom}}} \left(\Omega_{km}\varphi_{jm} + \Omega^*_{jm}\varphi^*_{km}\right), \tag{1}$$

$$\frac{dD_m}{dt} = -\gamma_D\left(1 + D_m\right) - 2\sum_{j=1}^{N_{\text{mode}}} \left(\Omega_{jm}\varphi_{jm} + \Omega^*_{jm}\varphi^*_{jm}\right), \tag{2}$$

$$\frac{d\varphi_{jm}}{dt} = -\gamma^{\varphi}_{jm}\varphi_{jm} + i\left(\omega^a_j - \omega_\sigma\right)\varphi_{jm} + \frac{\Omega^*_{jm}}{2}\left(D_m + 1\right) + \sum_{l=1}^{N_{\text{mode}}} \Omega^*_{lm} n_{jl} D_m. \tag{3}$$

In these equations n_{jj} is the photon number in the jth Bloch mode, n_{jk} is an interference term responsible for the flow of photons from the kth mode to the jth mode (where $j \neq k$), D_m is the population inversion of the mth atom, $\varphi_{jm} = -i\langle \hat{a}_j^+ \hat{\sigma}_m \rangle$ describes the energy flow between the mth atom and the jth mode, ω_j and γ_j correspond to the real and imaginary parts of the Bloch modes of the plasmonic structure, ω_σ and γ_D are the atom transition frequency and the relaxation rate of the population inversion of the atoms, $\gamma_{jm}^{\varphi} = \gamma_\sigma + \gamma_j + \gamma_D/2$, γ_σ is the relaxation rate of the phase of the atom polarization, and Ω_{jm} is the Rabi constant of coupling between the the jth mode and the mth atom, which can be expressed as

$$\Omega_{jm} = -\mathbf{d}_m \cdot \mathbf{E}_j(\mathbf{r}_m)/\hbar, \tag{4}$$

where $\mathbf{d}_m$ is the dipole moment of the mth atom at the transition frequency and $\mathbf{E}_j(\mathbf{r}_m)$ is the electric field "per quantum" in the jth Bloch mode at the position $\mathbf{r}_m$ of the mth atom (see the Appendix and Sec. 2 in the supplemental material for Ref. [13]). Every atom of the active medium has coordinates $\mathbf{r}_m$, which determine the Rabi constants of interaction between the atom and the Bloch modes of the plasmonic structure [see Eq. (4)]. This allows us to take into account the spatial distribution of the pumping and the population inversion within the active medium. Assuming that the time of the external pumping pulse lies in the femtosecond range and is much shorter than all the characteristic times of the plasmonic DFB laser, in our model, the ultrashort-pulse pumping is described as the initial condition, $D_m(0)$. For atoms lying inside the pump beam, the value of $D_m(0)$ is proportional to the pumping energy per unit area. The population inversions of the atoms whose coordinates lie outside the pump beam are -1 at the initial time. Note that the square of the Rabi constant is inversely proportional of the Bloch-mode volume and is proportional of the Purcell factor of the mode (see the Appendix).

Equations (1)–(3) generalize the rate equations widely used in laser theory [5]. In addition to the dynamics of the photon number in each mode and the population inversion of each atom, they describe energy flows between the active medium and the Bloch modes, and the interference between the EM fields of the different modes, n_{jk} [12].

For a quantitative description of the temporal dynamics of a plasmonic DFB laser under pulse pumping, we consider a laser based on a Au film perforated by a periodic array of nanosized holes and coated with a layer of the active medium (see Fig. 1). We consider that the thickness of the Au film is 100 nm, the diameter of the holes is 160 nm, and the distance between holes is 470 nm. The surface of the entire periodic plasmonic structure is $190 \times 190\ \mu\text{m}^2$. We consider that the transition frequency of the active medium, ω_σ, is close to the frequency of the second Bloch condition in the plasmonic structure; that is, $k_{\text{pl}}(\omega_\sigma) \approx G$, where k_{pl} is a wavevector of the mode in the plasmonic structure and G is a reciprocal lattice vector [11,13,15]. The linewidth of the active medium is about 100 nm. Similar plasmonic DFB lasers have been implemented in a number of experiments [8,11,15] and their parameters have been well studied [8,11,13,15].

The EM-field distribution of the Bloch modes of the plasmonic structure are found within the coupled-mode theory [11,13,15] (see also the Appendix), which describes the hybridization of modes of the system without holes through scattering on the holes. The scattering amplitudes for these modes are taken from Refs. [11,15]. The coupled-mode theory with such scattering amplitudes demonstrates good agreement with the experimental measurement of the band structure of the plasmonic nanohole array laser [11,15].

In the numerical simulations, we take into account 468 Bloch modes, which have different distributions of the EM field inside the cell of the plasmonic structure. The step of quantization of the Bloch wavevectors is determined by the size of the periodic plasmonic structure (see Ref. [13] and its supplemental material).

Using Eqs. (1)–(3), we simulate the time response to an ultrashort pumping pulse for different diameters of the pump beam. In Fig. 2(a) the dependence of the photon number on time is shown. As mentioned in Sec. I, there are three stages in the response of the system. In the first stage, the response of the system is determined by spontaneous emission in the active medium. The photon number in the plasmonic DFB laser is small. For the system considered, the duration of this stage (i.e., the delay time) is less than 1 ps. In the second stage, the photon number in the plasmonic laser rapidly increases due to stimulated emission in the active medium. This growth ceases with the saturation of the population inversion in the active medium. In the third stage, the photon number in the system decreases exponentially with time. We identify the total response time with the time when the number of photons in the system has decreased by a factor of 10 from its maximum value. This time is about 1 ps.

The dependence of the total photon number on time is qualitatively the same for different diameters of the pump beam. However, the response times have a nonmonotonic dependence on the size of the pump beam [see Fig. 2(b)]. It can be seen that there is a critical size of the pump beam at which the response time is a minimum. For the plasmonic DFB laser considered, the critical diameter of the pump beam is about 15 μm. As the pump-beam diameter decreases, the response time increases rapidly. With an increase in the diameter of the pump beam, the response time changes slowly. This kind of behavior of the plasmonic DFB laser occurs for different initial values of the population inversion of the active atoms. Thus, there is a diameter of the pump beam, d_{beam}^*, for which ultrafast light modulation in the plasmonic DFB laser is achieved.

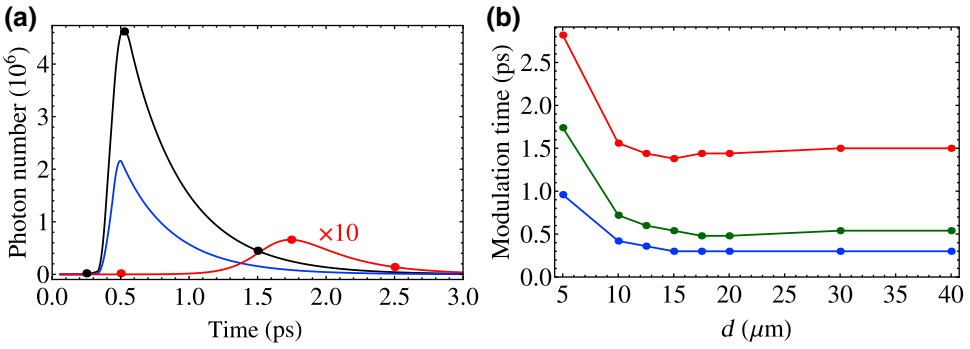

FIG. 2. (a) Dependence of the total photon number on the time for different diameters of the pump beam. The diameters are 20 μm (black line), 10 μm (blue line), and 5 μm (red line). (b) Dependence of the modulation times on the diameter of the pump beam. The blue line depicts the delay time, the green line depicts the time of the end of the second stage, and the red line depicts the total response time.

III. SINGLE-MODE APPROXIMATION

The existence of a critical size of the pump beam can be explained by the example of a single-mode model. To justify the single-mode approximation, we calculate the distribution of the electric field intensity over the area of the plasmonic DFB laser at different time (see Fig. 3). In Eqs. (1)–(3), we take into account several hundred of the Bloch modes of the plasmonic structure, which together form the EM-field distribution in the active medium. Numerical simulations show that this distribution does not change in the first and second stages of the system response. In other words, there is a dynamical balance between relaxation processes in the plasmonic structure, the propagation of the EM field outside the pumped area, and the stimulated amplification of the EM field inside the pumped area. When the diameter of the pump beam is larger than the critical value, $d_{\text{beam}} > d^*_{\text{beam}}$, the electric field is located inside the pumped region of the active medium [see Figs. 3(d)–3(f)]. In the opposite case, when $d_{\text{beam}} > d^*_{\text{beam}}$, the main part of the electric field is outside the pumped area [see Figs. 3(a)–3(c)]. However, in both cases, the spatial distribution of the electric field intensity remains almost unchanged during its temporal evolution.

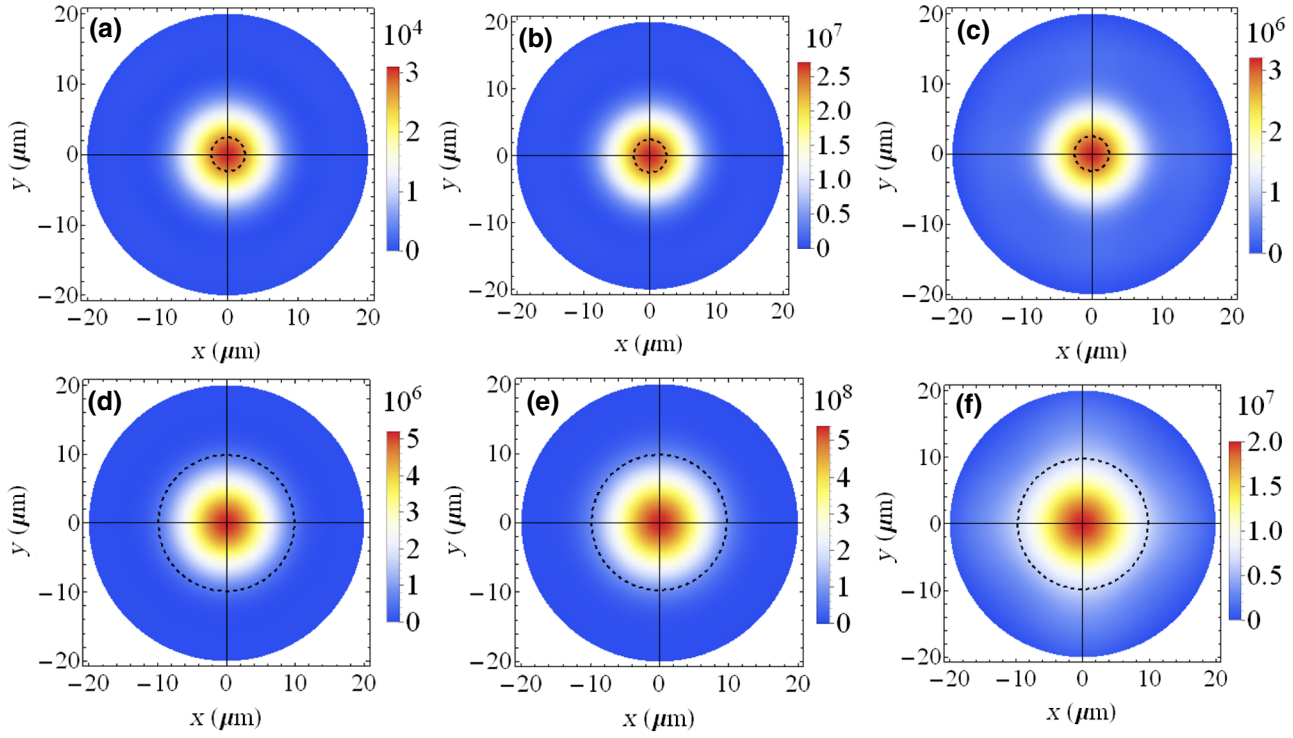

FIG. 3. a)–(c) Distribution of the EM-field intensity on the surface of the plasmonic DFB laser when the diameter of the pump beam $d_{\text{beam}} < d^*_{\text{beam}}$ at time 0.5 ps (a), 1.75 ps (b), and 2.5 ps (c). (d)–(f) Distribution of the EM-field intensity on the surface of the plasmonic DFB laser when the diameter of the pump beam $d_{\text{beam}} > d^*_{\text{beam}}$ at time 0.32 ps (d), 0.541 ps (e), and 1.5 ps (f). These times correspond to circles on the red curve and the black curve in Fig. 2(a), respectively. The dashed circles denote the boundaries of the pump beam.

We use the fact of the constancy of the EM-field distribution to construct a single-mode model. To do this, we assume that there is a single collective mode, the EM-field distribution of which coincides with the EM-field distribution found in the numerical simulations of the multimode problem. Furthermore, we assume that the pumped active medium interacts only with such a single collective mode. Within these approximations, the system dynamics can be described by the following system of equations [5]:

$$\dot{n} = -2\gamma_a n + 2N_{\text{at}}\Omega_R\varphi, \tag{5}$$

$$\dot{\varphi} = -\left(\gamma_a + \gamma_\sigma\right)\varphi + \Omega_R\left(2nD + D + 1\right)/2, \tag{6}$$

$$\dot{D} = -\gamma_D\left(D + 1\right) - 4\Omega_R\varphi, \tag{7}$$

where n is the number of photons in the collective mode, D is the mean population inversion of pumped atoms in the active medium, φ is the mean energy flow from the active medium to the collective mode, and N_{at} is the number of atoms in the active medium lying in the collective mode. We suppose that the relaxation rate of the EM field in the collective mode is equal to the characteristic relaxation rate of the modes of the plasmonic structure (i.e., $\gamma_a \simeq 10^{12}\ \text{s}^{-1}$). The finite size of the pump beam can lead to the appearance of edge effects and can influence the mode quality factor [21]. In the single-mode model, we do not take into account these effects for simplicity. We will further see that this simple model is in good agreement with the numerical simulations of Eqs. (1)–(3). The typical relaxation rate of the population inversion of the active medium is $\gamma_D \simeq 10^9\ \text{s}^{-1}$, while the phase relaxation rate is $\gamma_\sigma \simeq 10^{13}\ \text{s}^{-1}$. Thus, the phase relaxation rate is much larger than other relaxation rates, $\gamma_\sigma \gg \gamma_a, \gamma_D$. For this reason, one can adiabatically eliminate φ from Eqs. (5)–(7) and obtain the conventional rate equations

$$\dot{n} = -2\gamma_a n + N_{\text{at}}\Omega_R^2\left(2nD + D + 1\right)/\gamma_\sigma, \tag{8}$$

$$\dot{D} = -\gamma_D\left(D + 1\right) - 2\Omega_R^2\left(2nD + D + 1\right)/\gamma_\sigma. \tag{9}$$

As initial conditions we take $D(0) = 1$ and $n(0) = 0$ (i.e., all atoms are inverted and there are no photons in the mode). The temporal dynamics of such a system is well known [5]; it is shown in Fig. 4.

The dynamics of the photon number in the collective mode obtained with Eqs. (8)–(9) is similar to the behavior of the total photon number in the real plasmonic DFB laser [see Figs. 4(a) and 2(a)]. We observe three stages of the laser response, which are quantitatively similar to the stages in the real plasmonic DFB laser.

In the first stage, D is constant and n reaches stationary states at fixed D. Under this assumption the solution of Eq. (8) is

$$n\left(t\right) = \frac{N_{\text{at}}\Omega_R^2\left(D + 1\right)/\gamma_\sigma}{2N_{\text{at}}\Omega_R^2 D/\gamma_\sigma - 2\gamma_a}\left\{\exp\left[2\left(N_{\text{at}}\Omega_R^2 D/\gamma_\sigma - \gamma_a\right)t\right] - 1\right\} = \frac{\xi\left(D + 1\right)}{2\left(\xi - 1\right)}\left\{\exp\left[\left(\xi D - 1\right)2\gamma_a t\right] - 1\right\}, \tag{10}$$

where $\xi = N_{\text{at}}\Omega_R^2 D/\gamma_\sigma\gamma_a$ is the inverse threshold value of the pumping in the continuous-wave regime [23]. At the initial moment, $D \simeq 1$ and we have

$$n\left(t\right) = \frac{\xi}{\left(\xi - 1\right)}\left\{\exp\left[\left(\xi - 1\right)2\gamma_a t\right] - 1\right\}. \tag{11}$$

Substituting Eq. (11) into Eq. (9), we obtain

$$\dot{D} = -\gamma_D\left(1 + \eta\right)\left(D + 1\right) - \gamma_D\frac{2\xi\eta D}{\left(\xi - 1\right)} \times \left\{\exp\left[\left(\xi - 1\right)2\gamma_a t\right] - 1\right\}, \tag{12}$$

where we have put $\eta = 2\Omega_R^2/\gamma_D\gamma_\sigma$.

The second stage corresponds to the time when the exponential term in Eq. (12) is dominant, and the dynamics is strongly nonlinear. This nonlinear term describes the stimulated energy flow from the atoms to the collective mode. In this case, from Eq. (12) we obtain

$$\dot{D} = -\gamma_D\frac{2\xi\eta D}{\left(\xi - 1\right)}\exp\left[\left(\xi - 1\right)2\gamma_a t\right], \tag{13}$$

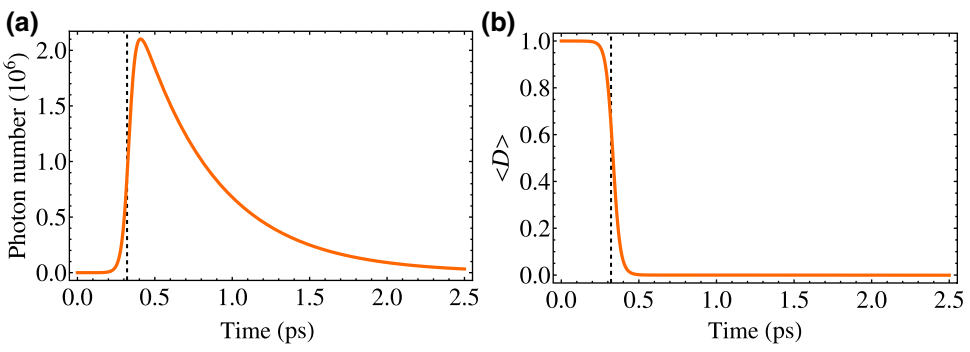

FIG. 4. Dependence of the photon number (a) and the population inversion of atoms (b) on time obtained from the single-mode model, Eqs. (8) and (9); the vertical dashed lines denote the delay time, t_{delay}, obtained with Eq. (16).

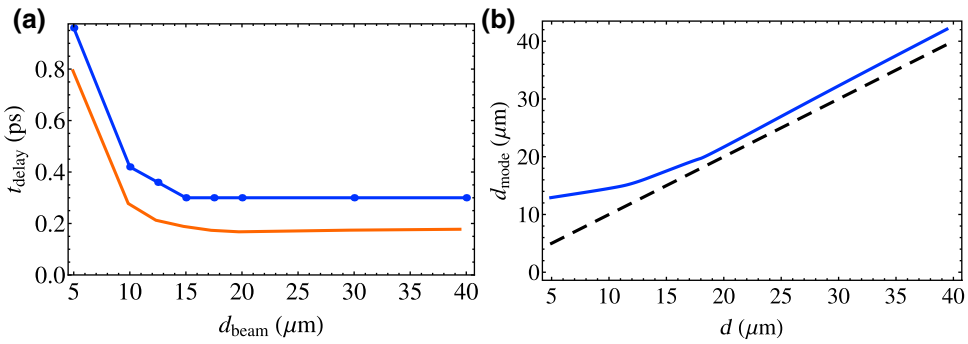

FIG. 5. (a) Dependence of the delay time on the pump-beam diameter. The solid blue line is obtained from numerical simulation with Eqs. (1)–(3) and the thick orange line is obtained from Eq. (16). (b) Dependence of the diameter of the collective mode on the pump-beam diameter (blue line). The dashed black line denotes the pump-beam diameter.

which has the solution

$$D(t) \simeq \exp\left(-\frac{\xi\eta\gamma_D}{(\xi-1)^2\gamma_a}\exp\left[(\xi-1)\,2\gamma_a t\right]\right) = \exp\left(-\frac{\xi^2}{N_{at}(\xi-1)^2}\exp\left[(\xi-1)\,2\gamma_a t\right]\right). \quad (14)$$

The characteristic time for D to change is

$$t_{delay} = (2\gamma_a)^{-1}(\xi-1)^{-1}\ln\left[N_{at}(\xi-1)^2/\xi^2\right]. \quad (15)$$

At this time, a sharp decrease of D appears [see Fig. 4(b)]. The assumption that the evolution of D is much slower than the evolution of n is valid when $t_{delay} \gg \gamma_a^{-1}\xi^{-1}$; that is, $\ln\left[N_{at}(\xi-1)^2/\xi^2\right] \gg 1$. When $\xi \gg 1$, the assumption is correct if $N_{at} \gg 1$, which is true for the system considered.

For $\xi \gg 1$, Eq. (15) simplifies to

$$t_{delay} = \gamma_\sigma \ln N_{at}/2N_{at}\Omega_R^2. \quad (16)$$

Figure 5(a) shows that the analytical approximation, Eq. (16), agrees well with the numerical simulation of the exact model, Eqs. (1)–(3). Let us analyze the dependence of the delay time, Eq. (16), on the size of the pumped area. The number of atoms depends quadratically on the diameter d_{beam} of the pump beam; that is, $N_{at} \sim d_{beam}^2$. In turn, the square of the Rabi constant is inversely proportional to the square of the diameter d_{mode}^2 of the collective mode; that is, $\Omega_R^2 \sim 1/d_{mode}^2$. So we have $t_{delay} \sim d_{mode}^2 \ln d_{beam}^2/d_{beam}^2$. The dependence of d_{mode} on d_{beam} is shown in Fig. 5(b).

It can be seen that there is a critical value, d_{beam}^*, of the diameter of the pump beam, which divides two different cases. When $d_{beam} > d_{beam}^*$, the electric field of the collective mode is localized inside the pump beam [see Figs. 3(d)–3(f)]. As a consequence, the mode diameter is proportional to the beam diameter; that is, $d_{mode} \sim d_{beam}$ [see Fig. 5(b)]. For this case, from Eq. (16) we have $t_{delay} \sim \ln d_{beam}$. This dependence is in agreement with a slow growth of the delay time of the DFB laser [see Fig. 2(b)]. When $d_{beam} < d_{beam}^*$, the electric field of the collective mode is localized outside the pump beam [see Figs. 3(a)–3(c)] and the mode size is determined by the characteristic propagation length of the EM field in the unpumped region. As a result, the mode diameter does not depend on the beam diameter, and $d_{mode} \sim$ const [see Fig. 5(b)]. In this case, $t_{delay} \sim \ln d_{beam}^2/d_{beam}^2$. This is in agreement with an increase of the delay time when the pump-beam diameter of the plasmonic DFB laser is reduced [see Fig. 2(b)]. The critical value d_{beam}^* corresponds to the characteristic propagation length of the EM field outside the pumped active medium and may be evaluated as $d_{beam}^* \sim v_{group}/\gamma_a$. For the parameters of the DFB laser we have $d_{beam}^* \sim 10$ μm, which is in agreement with the full model [see Fig. 2(b)]. Thus, because the delay time increases when $d_{beam} > d_{beam}^*$ and increases in the opposite case as well, we come to the conclusion that there is a critical value, approximately d_{beam}^*, for the diameter of the pump beam for which the response time is a minimum.

IV. CONCLUSION

To summarize, we study the temporal dynamics of a two-dimensional plasmonic DFB laser under ultrashort-pulse pumping. Relying on numerical simulations and analytical calculations, we show that the response time of such a laser for experimental parameters from Refs. [11,15] can be decreased to 1 ps, which corresponds to a modulation frequency of 1 THz. This value is close to the upper limit for plasmonic lasers (the total response time cannot be shorter than the time of the third stage, which is determined by the losses in the cavity, and is approximately 1 ps).

We show that the laser's response time can be shortened by optimization of the size of the pump beam, as a result of the consequent reduction of the delay time. The response time depends on the size of the pump beam for the following reason. The interaction of the laser modes with the pumped active medium results in the emergence of a single collective mode. If the size of the pump beam exceeds the propagation length of the EM waves, this collective mode is located in the pumped area. The response time then increase logarithmically with increasing pump-beam diameter. In contrast, when the mode is outside the pumped region, the response time is approximately

inversely proportional to the square of the pump-beam diameter, and so it increases rapidly as this diameter decreases from its critical value. It is interesting to note that the delay time, Eq. (16), resembles the dependence of the delay time of a superradiant burst [24–26]. Indeed, it is well known [24,25] that a system consisting of initially inverted atoms placed in a low-Q cavity (i.e., when $\gamma_a \gg \gamma_D$) exhibits a superradiant burst with the delay time, Eq. (16). In the plasmonic cavity, the inequality $\gamma_a \gg \gamma_D$ always holds, and for this reason, the superradiance problem and the problem that we investigate here have the same physical grounds. Further study of the relationship between these problems may be important in the context of creating ultrafast optoelectronic devices.

Finally, we show that there is a diameter of the pump beam, d^*_{beam}, necessary to achieve the shortest response time. This diameter is about the decay length of the EM field in the plasmonic structure, and for the plasmonic laser considered is approximately 15 μm. The existence of a critical pump-beam size provides the opportunity to reduce the energy consumption because further increase of the pump-beam size does not shorten the response time. In turn, if the area of the pump beam is small, there is an opportunity to reduce the size of the device. Thus, the results obtained pave the way to creating ultrafast optoelectronic devices based on plasmonic lasers with low power consumption that have the potential for on-chip integration.

ACKNOWLEDGMENT

This study was funded by the Russian Foundation for Basic Research (Project No. 18-32-00596) and Program No. 7 of the Presidium of RAS.

APPENDIX

To find the electric field $\mathbf{E}_j(\mathbf{r}_m)$ "per quantum," we equate the energy of one quantum to the energy of the EM field in the resonator:

$$\hbar\omega_j = \frac{1}{8\pi}\int_V \left(\frac{\partial \mathrm{Re}\left[\varepsilon(\omega,\mathbf{r})\omega\right]}{\partial\omega}\bigg|_{\omega=\omega_j} \left|\mathbf{E}_j(\mathbf{r})\right|^2 + \left|\mathbf{H}_j(\mathbf{r})\right|^2 \right) d^3\mathbf{r}, \tag{A1}$$

where $\varepsilon(\omega,\mathbf{r})$ is the dielectric constant.

In a two-dimensional periodic plasmonic structure whose surface is parallel to the xy plane, the electric and magnetic fields satisfy the Bloch condition:

$$\mathbf{E}_j(\mathbf{r}) = A_{0j}\exp\left(ik_{xj}x + ik_{yj}y\right)\mathbf{e}_j(x,y,z), \tag{A2}$$

$$\mathbf{H}_j(\mathbf{r}) = A_{0j}\exp\left(ik_{xj}x + ik_{yj}y\right)\mathbf{h}_j(x,y,z), \tag{A3}$$

where A_{0j} is a real normalization constant for the jth mode, $\mathbf{e}_j(x,y,z) = \mathbf{e}_j\left(x+L_x, y+L_y, z\right)$, $\mathbf{h}_j(x,y,z) = \mathbf{h}_j\left(x+L_x, y+L_y, z\right)$, and L_x and L_y are periods of the plasmonic structure along the x axis and the y axis, respectively.

The functions $\mathbf{e}_j(\mathbf{r})$ and $\mathbf{h}_j(\mathbf{r})$ can be found within the coupled-mode theory (see Refs. [11,15] and Sec. 2 in the supplemental material for Ref. [13]). In this approach, the eigenmodes of the plasmonic structure with holes are expressed as linear combinations of the eigenmodes of the plasmonic structure without holes [11,15]. The expansion coefficients are calculated through the scattering matrix, which contains the scattering amplitudes at angles 0°, ±90°, and 180°, and the effective refractive index of the plasmonic structure [11,15].

The eigenmodes of the plasmonic structure without holes are TM modes, similar to surface plasmons at the metal-dielectric interface [11,15]. These modes have an in-plane component of the magnetic field, $h_\parallel$, which is perpendicular to the direction of the mode's propagation and both an out-of-plane component, $e_\perp$, and an in-plane component, $e_\parallel$, of the electric field [11,15]. The in-plane component of the electric field, $e_\parallel$, is in the direction of the mode's propagation. The out-of-plane component of the electric field, $e_\perp$, is much greater than the in-plane component, $e_\parallel$ [11,15] and so it plays the main role in the interaction of the modes with the active medium.

The eigenmodes of the plasmonic structure with holes are found within the coupled-mode theory with the experimental values of the scattering amplitudes (see Refs. [11, 15] and Sec. 2 in the supplemental material for Ref. [13]). The coupled-mode theory with such scattering amplitudes demonstrates good agreement with the experimental measurement of the band structure of plasmonic nanohole arrays laser [11]. Near the transition frequency of the active medium, there are four different dispersion curves. The eigenmodes corresponding to different dispersion curves have various radiation losses and EM-field distributions inside the unit cell of the plasmonic structure (see Refs. [11,15] and Sec. 2 in the supplemental material for Ref. [13]). In particular, at the edge of the band gap, when the Bloch wavevectors $\left(k_{xj}, k_{yj}\right) = (0,0)$, the EM-field distributions in the modes from the different dispersion curves are as given in Table I (see Refs. [11,15] and Sec. 2 in the supplemental material for Ref. [13].)

The far-field radiation from the plasmonic structure arises mainly due to the scattering of $h_\parallel$ on the holes [11].

TABLE I. Eigenmodes of the plasmonic structure considered.

Number of the dispersion curve	$e_\parallel$	$h_\parallel$	$e_\perp$ (e_z)
1	$\sin Gx + \sin Gy$	$\sin Gx + \sin Gy$	$\cos Gx + \cos Gy$
2	$\sin Gx - \sin Gy$	$\sin Gx - \sin Gy$	$\cos Gx - \cos Gy$
3	$\cos Gy$	$\cos Gy$	$\sin Gy$
4	$\cos Gx$	$\cos Gx$	$\sin G$

For this reason, the modes that have a minimum value of $h_{\parallel}$ at the holes have smaller radiation losses than the modes that have a maximum value of $h_{\parallel}$ at the holes.

Suppose that the area under investigation contains an integral number N of plasmonic lattice cells. Then Eq. (A1) may be rewritten as

$$\hbar\omega_j = \frac{N}{8\pi}A_{0j}^2 \int_{V_{\text{cell}}} \left(\frac{\partial \text{Re}\left[\varepsilon(\omega,\mathbf{r})\omega\right]}{\partial\omega}\bigg|_{\omega=\omega_i} \left|\mathbf{e}_j\left(\mathbf{r}\right)\right|^2 + \left|\mathbf{h}_j\left(\mathbf{r}\right)\right|^2 \right) d^3\mathbf{r} \tag{A4}$$

where V_{cell} is the volume of the cell of the plasmonic lattice. As a result, we obtain that the normalization constant A_{0j} is expressed as

$$A_{0j} = \sqrt{\frac{\hbar\omega_j}{\frac{N}{8\pi}\int_{V_{\text{cell}}} \left(\frac{\partial \text{Re}[\varepsilon(\omega,\mathbf{r})\omega]}{\partial\omega}\Big|_{\omega=\omega_i} \left|\mathbf{e}_j\left(\mathbf{r}\right)\right|^2 + \left|\mathbf{h}_j\left(\mathbf{r}\right)\right|^2 \right) d^3\mathbf{r}}}. \tag{A5}$$

The Rabi constant between the jth mode and the mth atom, Ω_{jm}, is expressed as

$$\Omega_{jm} = -\mathbf{d}_m \cdot \mathbf{E}_j\left(\mathbf{r}_m\right)/\hbar, \tag{A6}$$

where $\mathbf{d}_m$ is the dipole moment of the mth atom of the active medium.

From Eqs. (A2) and (A7) we obtain

$$\Omega_{jm} = -\sqrt{\frac{8\pi\omega_j}{N\hbar\int_{V_{\text{cell}}} \left(\frac{\partial \text{Re}[\varepsilon(\omega,\mathbf{r})\omega]}{\partial\omega}\Big|_{\omega=\omega_i} \left|\mathbf{e}_j\left(\mathbf{r}\right)\right|^2 + \left|\mathbf{h}_j\left(\mathbf{r}\right)\right|^2 \right) d^3\mathbf{r}}} \times \left[\mathbf{d}_m \cdot \mathbf{e}_j\left(\mathbf{r}_m\right)\right] \exp\left(ik_{xj}x_m + ik_{yj}y_m\right). \tag{A7}$$

Thus, the Rabi constant may be rewritten as

$$\Omega_{jm} = \Omega_{0jm} \exp\left(ik_{xj}x_m + ik_{yj}y_m\right) f_j\left(\mathbf{r}_m\right), \tag{A8}$$

where Ω_{0jm} has the form

$$\Omega_{0jm} = -\sqrt{\frac{8\pi\omega_j \left|\mathbf{d}_m\right|^2 \left|\mathbf{e}_j\right|_{\max}^2}{N\hbar\int_{V_{\text{cell}}} \left(\frac{\partial \text{Re}[\varepsilon(\omega,\mathbf{r})\omega]}{\partial\omega}\Big|_{\omega=\omega_i} \left|\mathbf{e}_j\left(\mathbf{r}\right)\right|^2 + \left|\mathbf{h}_j\left(\mathbf{r}\right)\right|^2 \right) d^3\mathbf{r}}} = -\sqrt{\frac{8\pi\omega_j \left|\mathbf{d}_m\right|^2}{\hbar V_{j\,\text{th mode}}}}, \tag{A9}$$

where $\left|\mathbf{e}_j\right|_{\max}$ is the maximum value of the periodic function $\left|\mathbf{e}_j\left(\mathbf{r}\right)\right|$ and $V_{j\text{th mode}} = \frac{\int_{V_{\text{cell}}} \left(\frac{\partial \text{Re}[\varepsilon(\omega,\mathbf{r})\omega]}{\partial\omega}\Big|_{\omega=\omega_i} \left|\mathbf{e}_j\left(\mathbf{r}\right)\right|^2 + \left|\mathbf{h}_j\left(\mathbf{r}\right)\right|^2 \right) \times d^3\mathbf{r}}{\left|\mathbf{e}_j\right|_{\max}^2}$ is the mode volume of the jth mode. Thus, $\Omega_{0jm}^2 \sim 1/V_{j\text{th mode}}$ and, as a consequence, is proportional to the Purcell factor of the jth mode [2]. Also, $f_j\left(\mathbf{r}_m\right) = \left[\mathbf{d}_m \cdot \mathbf{e}_j\left(\mathbf{r}_m\right)\right]/\left(\left|\mathbf{d}_\mathbf{m}\right|\left|\mathbf{e}_j\right|_{max}\right)$ is a periodic function with plasmonic-lattice-cell period. The functions $f_j\left(\mathbf{r}_m\right)$ for the modes lying in the different bands are orthogonal to each other. The orthogonality arises due to difference in the EM-field distributions within the cell of the plasmonic structure for the modes lying in the different bands (see Table I).

[1] Konstantinos S. Daskalakis, Aaro I. Väkeväinen, Jani-Petri Martikainen, Tommi K. Hakala, and Päivi Törmä, Ultrafast pulse generation in an organic nanoparticle-array laser, Nano. Lett. **18**, 2658 (2018).

[2] W. Zhou, M. Dridi, J. Y. Suh, C. H. Kim, D. T. Co, M. R. Wasielewski, G. C. Schatz, and T. W. Odom, Lasing action in strongly coupled plasmonic nanocavity arrays, Nat. Nanotech. **8**, 506 (2013).

[3] Hatice Altug, Dirk Englund, and Jelena Vučković, Ultrafast photonic crystal nanocavity laser, Nat. Phys. **2**, 484 (2006).

[4] D. Englund, H. Altug, B. Ellis, and J. Vučković, Ultrafast photonic crystal lasers, Laser Photon. Rev. **2**, 264 (2008).

[5] A. E. Siegman, *Lasers* (University Science Books, Mill Valley, CA, 1986), p. 654.

[6] Larry A. Coldren, Scott W. Corzine, and Milan L. Mashanovitch, *Diode Lasers and Photonic Integrated Circuits* (John Wiley & Sons, New Jersey, 2012), Vol. 218.

[7] J. W. Scott, B. J. Thibeault, C. J. Mahon, L. A. Coldren, and F. H. Peters, High modulation efficiency of intracavity contacted vertical cavity lasers, Appl. Phys. Lett. **65**, 1483 (1994).

[8] F. Beijnum, P. J. Veldhoven, E. J. Geluk, M. J. A. Dood, G. W. 't Hooft, and M. P. van Exter, Surface Plasmon Lasing Observed in Metal Hole Arrays, Phys. Rev. Lett. **110**, 206802 (2013).

[9] A. H. Schokker and A. F. Koenderink, Lasing at the band edge of plasmonic lattices, Phys. Rev. B **90**, 155452 (2014).

[10] X. Meng, J. Liu, A. V. Kildishev, and V. M. Shalaev, Highly directional spaser array for the red wavelength region, Laser Photon. Rev. **8**, 896 (2014).

[11] V. T. Tenner, A. N. van Delft, M. J. A. de Dood, and M. P. van Exter, Loss and scattering of surface plasmon polaritons on optically-pumped hole arrays, J. Opt. **16**, 114019 (2014).

[12] A. A. Zyablovsky, E. S. Andrianov, I. A. Nechepurenko, A. V. Dorofeenko, A. A. Pukhov, and A. P. Vinogradov, Approach for describing spatial dynamics of quantum light-matter interaction in dispersive dissipative media, Phys. Rev. A **95**, 053835 (2017).

[13] Nikita E. Nefedkin, Alexander A. Zyablovsky, Evgeny S. Andrianov, Alexander A. Pukhov, and Alexey P. Vinogradov, Mode cooperation in a two-dimensional plasmonic distributed-feedback laser, ACS Photonics **5**, 3031 (2018).

[14] A. V. Dorofeenko, A. A. Zyablovsky, A. P. Vinogradov, E. S. Andrianov, A. A. Pukhov, and A. A. Lisyansky, Steady state superradiance of a 2d-spaser array, Opt. Express **21**, 14539 (2013).

[15] V. T. Tenner, M. J. A. de Dood, and M. P. van Exter, Measurement of the phase and intensity profile of

surface plasmon laser emission, ACS Photonics **3**, 942 (2016).

[16] A. A. Zyablovsky, I. A. Nechepurenko, E. S. Andrianov, A. V. Dorofeenko, A. A. Pukhov, A. P. Vinogradov, and A. A. Lisyansky, Optimum gain for plasmonic distributed feedback lasers, Phys. Rev. B **95**, 205417 (2017).

[17] P. Melentiev, A. Kalmykov, A. Gritchenko, A. Afanasiev, V. Balykin, A. Baburin, E. Ryzhova, I. Filippov, I. Rodionov, I. A. Nechepurenko, A. V. Dorofeenko, I. Ryzhikov, A. P. Vinogradov, A. A. Zyablovsky, E. S. Andrianov, and A. A. Lisyansky, Plasmonic nanolaser for intracavity spectroscopy and sensorics, Appl. Phys. Lett. **111**, 213104 (2017).

[18] A. H. Schokker, and A. F. Koenderink, Statistics of randomized plasmonic lattice lasers, ACS Photonics **2**, 1289 (2015).

[19] A. Yang, T. B. Hoang, M. Dridi, C. Deeb, M. H. Mikkelsen, G. C. Schatz, and T. W. Odom, Real-time tunable lasing from plasmonic nanocavity arrays, Nat. Commun. **6**, 6939 (2015).

[20] A. Yang, Z. Li, M. P. Knudson, A. J. Hryn, W. Wang, K. Aydin, and T. W. Odom, Unidirectional lasing from template-stripped two-dimensional plasmonic crystals, ACS Nano **9**, 11582 (2015).

[21] T. K. Hakala, H. T. Rekola, A. I. Väkeväinen, J.-P. Martikainen, M. Nečada, A. J. Moilanen, and P. Törmä, Lasing in dark and bright modes of a finite-sized plasmonic lattice, Nat. Commun. **8**, 13687 (2017).

[22] Danqing Wang, Ankun Yang, Weijia Wang, Yi Hua, Richard D. Schaller, George C. Schatz, and Teri W. Odom, Band-edge engineering for controlled multi-modal nanolasing in plasmonic superlattices, Nat. Nanotechnol. **12**, 889 (2017).

[23] M. O. Scully and M. S. Zubairy, *Quantum Optics* (Cambridge University Press, Cambridge, 1997).

[24] Michel Gross and Serge Haroche, Superradiance: An essay on the theory of collective spontaneous emission, Phys. Rep. **93**, 301 (1982).

[25] Anatolii V. Andreev, Vladimir I. Emel'yanov, and Yu. A. Il'inskii, Collective spontaneous emission (dicke superradiance), Sov. Phys. Usp. **23**, 493 (1980).

[26] N. E. Nefedkin, E. S. Andrianov, A. A. Pukhov, and A. P. Vinogradov, Superradiance enhancement by bad-cavity resonator, Laser Phys. **27**, 065201 (2017).